To be published in Optics Letters:

Title: On the coupling of two helical waveguides

Authors: Mingjie Cui,Zhuo Wang,Changyuan Yu

Accepted: 25 September 24

Posted 27 September 24

DOI: https://doi.org/10.1364/OL.533849

On the coupling of two helical circular waveguides

MINGJIE CUI,[1] ZHUO WANG,[2] AND CHANGYUAN YU[1,3,*]

[1]*Photonics Research Institute, Department of Electrical and Electronic Engineering, The Hong Kong Polytechnic University, Kowloon, Hong Kong*

[2]*Guangdong Provincial Key Laboratory of Nanophotonic Functional Materials and Devices, School of Information and Optoelectronic Science and Engineering, South China Normal University, Guangzhou 510006, China*

[3]*The Hong Kong Polytechnic University Shenzhen Research Institute, Shenzhen 518057, China*

**Corresponding author: changyuan.yu@polyu.edu.hk*

Received XX Month XXXX; revised XX Month, XXXX; accepted XX Month XXXX; posted XX Month XXXX (Doc. ID XXXXX); published XX Month XXXX

Coupling between optical waveguides has always been an important topic. By using the finite element method based on a helicoidal coordinate system, we present a detailed study of the couplings between two helical coupled circular waveguides, showing several important aspects that were not found in the previous studies. Our numerical results show that for the two-fold rotationally symmetric cases, intersections will appear in the effective index curves of the two composite modes with the increasing twist rate and we have found that this is related to the different increases of the composite modes in the helical path and the emergence of high-order harmonics. Further, for the one-fold rotationally symmetric structures formed by the two waveguides with the same radical but different azimuthal positions, as the twist rate increases, we observe the emerging asymmetric modal distributions of the composite modes, indicating that couplings between the two waveguides are no longer equivalent. © 2024 Optical Society of America

Light can travel from one waveguide to another when two waveguides are placed close enough. This is known as the coupling between two waveguides, which is one of the basic behaviors of light, and it can be described by the coupled-mode theory developed in the early 1970s [1]. Studies on the couplings between optical waveguides have greatly promoted the development of optical waveguide devices such as sensors [2], couplers [3], and beam splitters [4]. Later, in the 1980s, a helical-core fiber was reported and it was demonstrated that circular birefringence and single-mode transmission at large normalized frequencies can be achieved by the fiber [5]. Researchers have come to realize that twisting a fiber can offer an additional degree of freedom for controlling light. The growing interest in helical waveguides and the mode couplings within them has further developed the application of helical fibers. They can be used as polarizers [6,7], vortex generators [8-10], and fiber lasers [11,12].

Recently, a circular polarization beam splitter has been proposed, which involves the coupling between two cores in a helically twisted twin-core photonic crystal fiber [13]. In the presented fiber coupler, it can be observed that the coupling lengths increase with twist rate but the cause for this increase remains unclear in the paper. Actually, an earlier study involving light transfer between two twisted fibers revealed that this phenomenon is related to the centrifugal effect [14]. In 2021, the study of helical Bloch modes in coupled spiraling optical waveguides also mentioned that the coupling between cores can be reduced due to the centrifugal effect in the twisted fibers [15]. The analysis in [14,15] can help explain the increases in the coupling length shown in [13] to some extent. However, this interpretation may not be comprehensive enough because it does not intuitively show the effect in terms of coupling length/coefficient related to the composite modes.

In this letter, we carry out numerical simulations on the coupling characteristics of two coupled helical circular waveguides by using the finite element method (FEM) based on a helicoidal coordinate system. The obtained results show that the changes in couplings with twist rates are related to the different increases in the helical path of the composite modes and the emergence of high-order harmonics as well as the broadening of the modal field. Further, we report on the emerging asymmetric modal distributions of the composite modes with the increasing twist rate in the case of the two coupled waveguides placed at the same radical but different azimuthal positions.

Figure 1 shows the cross-section and the formation of two helical circular waveguides. for simplicity, they can be treated as two helical cores in an optical fiber. The core diameters d=6 μm are used through all the simulations, α is the twist rate, and ρ is the distance from cores to the fiber center (Z axis), which would take different values in the following simulations. To ensure the single-mode transmission in the cores, the core index is set to 0.01 higher than the cladding and the cladding silica index is around 1.444 at the operating wavelength λ=1.55 μm. The modal characteristics of the helical waveguides are obtained by using the FEM based on the helicoidal coordinate system as presented in [16]. Note that the outermost region is surrounded by a perfectly matched layer (PML) which can be applied to twisted fibers [17].

To study the coupling characteristics of coupled waveguides, it is important to introduce the coupling length which can be well defined as [18]:

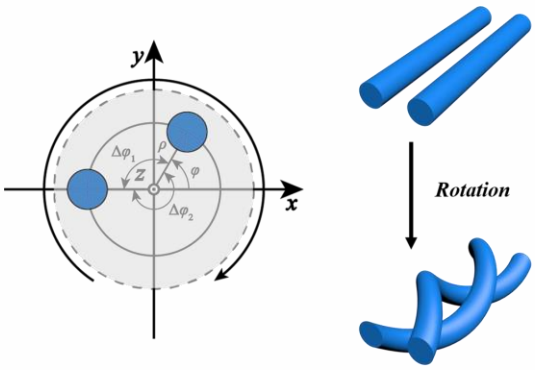

Fig. 1. Cross-section (left) and sketch (right) of the formation of two helical circular waveguides. The angle φ denotes the azimuthal position of the core on the right. The Curved arrow shows the twist direction.

$$L_c = \frac{\pi}{\left|\beta_{even} - \beta_{odd}\right|}, \tag{1}$$

where β_{even} and β_{odd} are propagation constants of the symmetric mode and the antisymmetric mode, respectively, also known as even and odd modes. Firstly, for a two-fold rotationally symmetric case (φ=0), we calculated the effective indices of the composite modes versus $\alpha\rho$ in the helical frame using FEM directly with a relatively small core offset ρ = 4 μm as shown by the solid lines in Fig. 2(a). Note that modes obtained from the helical frame will be divided into two orthogonal circularly polarized modes, left- and right-circularly polarized (LCP and RCP) modes. Unless specified, only the RCP modes, with the same handedness as the helical core, are shown in this letter since the difference between the two orthogonal modes is very minor in the coupling characteristics.

As shown by solid lines in Fig. 2(a), one can see the effective indices increase with twist rate, which indicates that modes travel a longer helical path. As the twist rate gets higher, the difference between even and odd modes is narrowing in the effective index. It means that coupling between cores is weakened, simultaneously, appearing to be an increase in the coupling length as shown in the lower subgraph. This increase is in agreement with the relevant result shown in [13] and it can be explained by a centrifugal effect of the modal field caused by the fiber twist from the perspective of [14,15]. As shown in Fig. 2(b), the centrifugal effect manifests as the modal field moving outward. As we continue to observe, it can be seen that the two curves cross at 0.0471 and the odd mode exceeds the even mode with increasing twist rate resulting in a peak appearing in the coupling length However, this has not been discussed further in previous studies. Particularly, in this case, the decrease in coupling length after the peak does not seem to be intuitively explained by the field profiles moving outward radically. For further analysis, we apply the coupled-mode analysis to the two helical cores. The propagation constant and the modal field for an isolated helical core are calculated first by FEM. And then, the propagation constant of composite modes can be approximated by [19]:

$$\beta_{even/odd} = \beta_{ave} \pm \sqrt{\delta^2 + \kappa^2}, \tag{2}$$

one where $\beta_{ave} = (\beta_1+\beta_2)/2$ is the average value of the propagation of two isolated helical cores, $\delta = (\beta_1-\beta_2)/2$ is the phase mismatch factor,

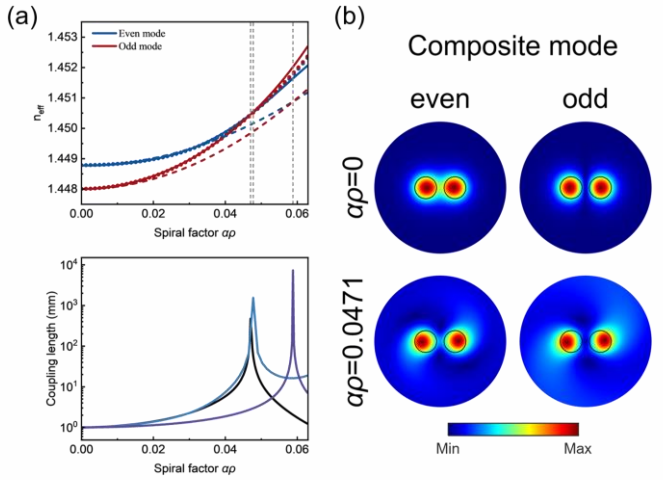

Fig. 2. (a) Effective index of the composite modes (upper) evaluated by direct FEM (solid lines), coupled-mode analysis (dotted lines), and Eq. (4) (dashed lines), in the laboratory frame, and the corresponding coupling lengths (lower) represented by black, blue, and purple lines, respectively. (b) Modal distributions of the composite modes.

and with normalized optical power, coupling coefficient $\kappa = \sqrt{\kappa_{12}\kappa_{21}}$ can be well defined by:

$$\kappa_{pq} = \frac{\omega\varepsilon_0}{4}\int_{-\infty}^{\infty} E_p^* \cdot \Delta\varepsilon E_q dA, \tag{3}$$

where ω is the angular frequency, ε_0 is the permittivity of vacuum, and for waveguides treated in the helical coordinate system, $\Delta\varepsilon$ is the perturbation of the permittivity tensor, as an addition of the second helical core. By calculating β_1 and β_2 of the two cores in the helical frame separately and κ the coupling coefficient, the calculated effective index of the composite modes using Eq. (2) is shown by the dotted line in Fig. 2(a). It is observable that the intersection at ~0.0478 can also be seen in the dot lines and correspondingly, a peak occurs in the coupling length by the blue line shown in the lower subgraph. Despite the difference in magnitude at the high twist rate region, the solid line and the dotted line are consistent, which implies that the coupled-mode theory is still a good approximation in the helical frame. Nevertheless, we have found that it is possible to describe the intersection analytically. According to [15, 20-22], one can know that the effective index of helical waveguides can be described analytically by proper approximation. Generally, the analytical expressions contain two parts: the increase in the helical path and the angular momentum correction term. Similarly, the effective index of the composite modes for the two coupled helical waveguides can take the following form:

$$n_{even/odd}' = n_{even/odd}\sqrt{\left(1+\alpha^2\rho^2\right)} + \Delta n, \tag{4}$$

where $n_{even/odd}$ is the effective index of composite modes in the untwisted waveguides, ρ often refers to the core offset to the fiber center, and Δn denotes the deviation from the FEM results, which contains the correction terms. This term will be neglected when referring to the use of Eq. (4). For composite

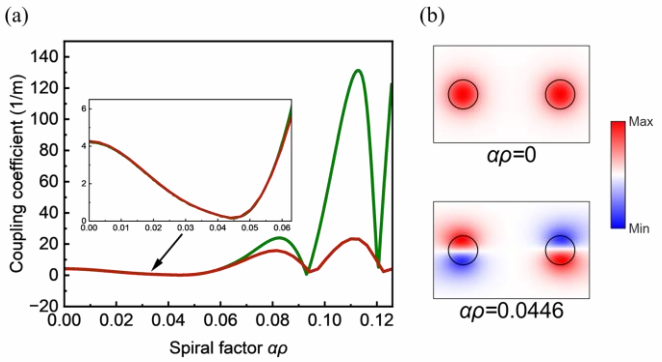

Fig. 3. (a) Real part of coupling coefficients κ evaluated by direct FEM (green) and coupled-mode analysis (red). (b) Selected transverse electric fields of even mode.

modes of the two cores, the deviation between the position where the maximum of the modal field is located and the core center needs to be taken into account especially when the two cores are close. This suggests that ρ should be equal to the effective modal offset ρ_{eff} which represents the position of maximum of the modal field. In this simulation, the effective modal offsets ρ_{eff} are ~3.67 μm and ~4.29 μm for the even and the odd modes when the core offset equals 4 μm. As depicted by the dashed lines (upper subgraph) and the purple solid line (lower subgraph) in Fig. 2(a), one can see the effective indices calculated by Eq. (4) and the corresponding coupling length has the same trend with the two previous results, and the intersection between the dashed lines appears at 0.0588. The deviation from the previous results can be mainly attributed to high-order corrections. Note that the deviation can also be improved by taking the influence of the centrifugal effect on the ρ_{eff} into account [23]. This simple analytical result reveals that the intersection between the composite modes in the effective index is a result of the differential increase in the helical path whether the high-order corrections are taken into account or not, which neatly illustrates that intrinsically, the weakening of coupling between cores is caused by the difference in the helical path in terms of the composite modes. Moreover, the intersection between effective indices of the composite mode does not mean coupling between the two modes for no extrema show at the position corresponding to the loss spectrum (see Supplement 1). This could be a result of the angular momentum mismatch of the two modes.

For the next, we show the coupling characteristics by calculating the coupling coefficients κ with respect to $\alpha\rho$ when the core offset is larger with ρ = 10 μm. As shown in Fig. 3(a) by the green line, with the increasing twist rate, the initial drop in κ indicates the weakening of coupling, clearly consistent with the above discussion as depicted in the inset. However, one can observe that the κ rises and drops alternately acting like a cosine function that takes the absolute value in the relatively high $\alpha\rho$ region, which can no longer be described analytically. By modal analysis, as shown in Fig. 3(b), we have found that this is actually caused by the emergence of high-order harmonics and the broadening of the modal fields with the increase of $\alpha\rho$ [24]. Likewise, the coupled-mode analysis is also applied and the calculated κ is shown by the red line. It can be seen that the coupling coefficient calculated by Eq. (3) is still in good agreement with the result evaluated

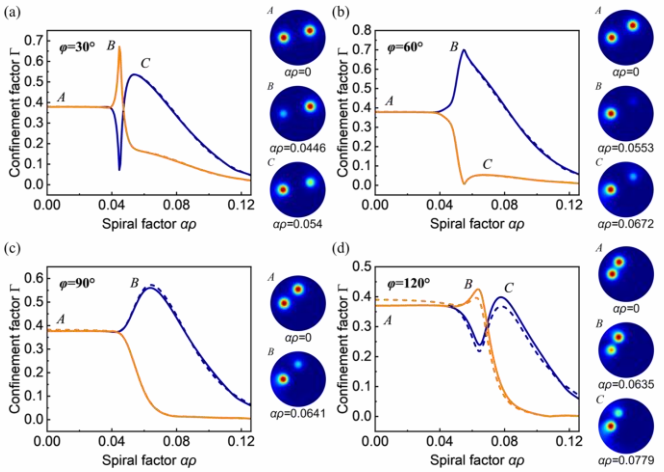

Fig. 4. The calculated Confinement factor Γ versus $\alpha\rho$ for φ=30°(a), 60°(b), 90°(c), and 120°(d). Solid and dashed lines represent even and odd modes while blue and yellow indicate core 1 and 2, respectively. Insets: Selected modal distributions of even mode.

directly from FEM, especially in the low twist rate region as shown by the inset. As to the mismatch in magnitude in the relatively high twist rate region, we attribute this to an error in the perturbation approximation. Thus, the curves are generally consistent in trend. Besides, it is worth noting that the relationship $\kappa_{12} = \kappa_{21}^*$ gradually turns into $\kappa_{12} = \kappa_{21}$ with the increasing twist rate (see Supplement 1). Further, one can see two sharp declines in the vicinity of $\alpha\rho$ at ~0.09 and ~0.12 suggesting that two intersections will show in the effective index curves of two composite modes. Similar to the previous case, no couplings between the two composite modes are observed at the two intersections as well (see Supplement 1).

Subsequently, we study a more general case. By placing one core at different azimuthal positions, the whole cross-section is deduced to an asymmetric (one-fold rotationally symmetric) structure. The core on the right rotates by the angle φ with respect to the initial position and the angular deviations $\Delta\varphi_1$ and $\Delta\varphi_2$ will be different. With the growing twist rate, we have observed that an asymmetric coupling effect occurred, showing that couplings between the two cores are no longer equivalent. As illustrated in Fig. 4, optical power change in the cores is expressed by the confinement factor Γ and it is well defined as:

$$\Gamma = \frac{P_{core}}{P_{total}} = \frac{\int_{core} \langle S_z \rangle dA}{\int_{cross-section} \langle S_z \rangle dA}, \tag{5}$$

where $\langle S_z \rangle$ is the longitudinal component of time-averaged Poynting vector. The calculated Γ_1 and Γ_2 denote the confinement factor of the two cores from left to right. One can see that optical power in both cores changes differently with increasing twist rates for different φ. As shown in Fig. 4(a), for φ=30° it is evident that Γ_1 and Γ_2 begin to split at around $\alpha\rho$=0.04. With the increase of twist rate, Γ_1 drops dramatically to a minimum lower than 0.1 whereas Γ_2 rises to a maximum close to 0.7 showing an asymmetric mode profile marked by *B*. After the sharp peaks, Γ_2 drops and Γ_1 rises showing a new mode profile but with Γ_1 greater than Γ_2 this time. Particularly,

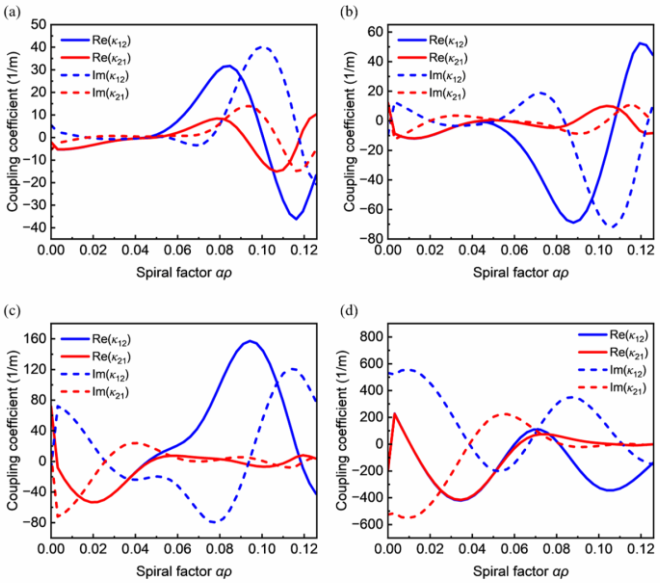

Fig. 5. The real and imaginary parts of coupling coefficients calculated by using the coupled-mode analysis versus $\alpha\rho$ for φ=30°(a), 60°(b), 90°(c), and 120°(d).

the sharp peaks here can be considered as couplings between the composite modes (see Supplement 1). Similarly, Γ_1 and Γ_2 separate near the same $\alpha\rho$ but the obvious difference is no case of Γ_1 greater than Γ_2 with increasing twist rate as shown in Fig. 4(b) for φ=60°. Despite that, Γ_2 still undergoes a minimum in the vicinity of ~0.055 exhibiting a clear change of strength in power as depicted by modal distributions marked by *B* and *C*. As for φ=90° one can see that Γ_2 is almost monotonically decreasing and Γ_1 is always higher since the splitting. When it comes to φ=120°, it is not difficult to see that the shape of the curves shown in Fig. 4(d) is quite similar to that in Fig. 4(a). One can see the maximum of Γ exchanged in turn from 0.06 to 0.08. And then both Γ_1 and Γ_2 decrease but still Γ_1 is greater than Γ_2, with the growing twist rate. Overall, the asymmetric distributions of intensity described above suggest that waveguides arranged in such ways can contribute to the special design of fiber couplers. Furthermore, to get a better perspective, we also show the calculated coupling coefficients for these cases. As shown in Fig. 5, although the coupling coefficients change with $\alpha\rho$ significantly, the κ_{12}=κ_{21}^* can be considered true for relatively low twist rate region (i.e. $\alpha\rho$<0.04). However, as the twist rate increases, it is evident that κ_{12} is no longer equal to κ_{21}* and this could be attributed to the effect of the emergence of high-order harmonics and the broadening of the modal fields on the overlap integral. Note that the abrupt change of coupling coefficients near $\alpha\rho$=0 is caused by the change of coordinate systems. Moreover, the calculated κ in these cases shares a similar trend with the result shown in Fig. 3(a) (See supplement 1).

In conclusion, we have shown the couplings between two helical coupled circular waveguides in detail. For a two-fold rotationally symmetric structure formed by two helical coupled waveguides, with increasing twist rate, the initial weakening appears in coupling between the cores, and the resulting intersections occurring between even and odd modes in the effective index can be well expressed by Eq. (4) showing that the trend is in good agreement with results evaluated from direct FEM and coupled-mode analysis when the two waveguides are relatively close. This indicates that in terms of composite modes, intrinsically, the proximity between two composite modes in the effective index can be understood as the length of the helical path they traveled is different due to the difference in location of the modal maxima regardless of the high-order corrections. For larger core offset we have pointed out that the oscillation shown in the coupling coefficient is a result of the emergence of high-order harmonics and the broadening of the modal field. For one-fold rotationally symmetric structures formed by the waveguides with the same distance to the fiber axis but different azimuthal positions, we observed the asymmetric distributions of the composite mode. Meanwhile, couplings between the two cores are no longer equivalent to each other at some twist rates. This implies that in these cases one will obtain $\kappa_{12} \neq \kappa_{21}^*$ even though β_1=β_2 holds all the time, which makes it an interesting case for the coupled-mode analysis. Further, we also observed that power in the core that rotates toward a smaller angular deviation $\Delta\varphi_1$ is always higher than the other when in the high twist rate range (See supplement 1). Nevertheless, field distributions of the composite mode will be inverse if we change the twist direction. We believe our findings provide a new perspective for the special designs of waveguide couplers and multi-waveguide systems, and the studies of optical waveguide interactions.

Funding. This work is supported by the Hong Kong Research Grants Council (GRF Project No. 15209321).

Disclosures. The authors declare no conflicts of interest.

Supplemental document. See Supplement 1 for supporting content.

References

1. D. Marcuse, *Light Transmission Optics* (Van Nostrand, 1972).
2. C. Caucheteur, J. Villatoro, F. Liu, *et al*., Adv. Opt. Photonics **14**, 1 (2022).
3. M. J. F. Digonnet and H. J. Shaw, IEEE J. Quantum Electron. **18**, 746–754 (1982).
4. L. Zhang, C. Yang, C. Yu, *et al.*, J. Lightwave Technol. **23**, 3558 (2005).
5. R. D. Birch, Electron. Lett. **23**, 50 (1987).
6. V. I. Kopp, V. M. Churikov, J. Singer, *et al.*, Science **305**, 74 (2004).
7. V. I. Kopp, J. Park, M. Wlodawski, *et al.*, J. Lightwave Technol. **32**, 605 (2014).
8. C. N. Alexeyev, A. N. Alexeyev, B. P. Lapin, *et al*., Phys. Rev. A **88**, 063814 (2013).
9. X. M. Xi, G. K. L. Wong, M. H. Frosz, *et al*., Optica **1**, 165 (2014).
10. T. Fujisawa and K. Saitoh, Opt. Express **30**, 24565-24578 (2022).
11. X. Ma, C. Zhu, I.-N. Hu, *et al.*, Opt. Express **22**, 9206 (2014).
12. X. Zeng, P. St.J. Russell, Y. Chen, *et al.*, Laser Photonics Rev. **17**, 2200277 (2023).
13. J. E. Usuga-Restrepo, W. M. Guimaraes, and M. A. R. Franco, Opt. Fiber Technol. **58**, 102285 (2020).
14. S. Longhi, J. Phys. B **40**, 4477 (2007).
15. Y. Chen and P. St.J. Russell, J. Opt. Soc. Am. B **38**, 1173 (2021).
16. A. Nicolet, F. Zolla, Y. O. Agha, *et al*., COMPEL **27**, 806 (2008).
17. A. Nicolet, F. Zolla, Y. O. Agha, *et al.*, Waves Random Complex Media **17**, 559 (2007).
18. K. Okamoto, Fundamentals of Optical Waveguides.
19. Z. Zhang, Y. Shi, B. Bian, *et al*., Opt. Express **16**, 1915 (2008).
20. X. Ma, C.-H. Liu, G. Chang, *et al*., Opt. Express **19**, 26515 (2011).
21. P. St. J. Russell and Y. Chen, Laser Photonics Rev. **17**, 2200570 (2023).
22. J. Bürger, A. C. Valero, T. Weiss, *et al*, Phys. Rev. B **109**, 165301 (2024).
23. M. Napiorkowski and W. Urbanczyk, Opt. Express **22**, 23108 (2014).
24. M. Napiorkowski and W. Urbanczyk, J. Opt. **18**, 055601 (2016).